Wuhan University
Journal of Natural Sciences

2026, Vol.31 No.2, 133-145

Article ID 1007-1202(2026)02-0133-13 DOI https://doi.org/10.1051/wujns/2026312133

Cite this article: LIU Jian, CHEN Zhenghu, CAI Wei, *et al*. Efficacy and Mechanism of Common Chemical Agents on *Limnoperna fortunei* in Hydraulic Engineering[J]. *Wuhan Univ J of Nat Sci*, 2026, 31(2): 133-145.

Efficacy and Mechanism of Common Chemical Agents on *Limnoperna fortunei* in Hydraulic Engineering

□ **LIU Jian[1,2], CHEN Zhenghu[3], CAI Wei[3], WANG Yingcai[1,2], TIAN Nana[1,2], GUO Wensi[1,2], LI Tiancui[1,2†]**

1. Ecology and Environment Monitoring and Scientific Research Center, Changjiang Basin Ecology and Environment Administration, Ministry of Ecology and Environment, Wuhan 430010, Hubei, China;

2. Key Laboratory of Aquatic Organisms Monitoring and Assessment of the Changjiang Basin, Ministry of Ecology and Environment (under construction), Wuhan 430010, Hubei, China;

3. China Yangtze Power Co., Ltd., Yichang 430014, Hubei, China

Abstract: *Limnoperna fortunei* (*L. fortunei*) is a major fouling organism in hydraulic systems, where chemical control remains a common practice. This study evaluated the molluscicidal efficacy and mechanisms of eight chemical agents including copper sulfate ($CuSO_4$), chloramine, sodium hypochlorite (NaClO), salicylic acid, glyphosate, chitosan-based flocculant, nicotinoyl aniline sulfate ($C_{12}H_{10}N_2O \cdot H_2SO_4$, abbreviated as NS) and polyquaternium. The results show that the order of toxicity from high to low was NS > $CuSO_4$ > NaClO > polyquaternium > salicylic acid > glyphosate > chloramine > chitosan-based flocculant. Notably, NS (2 mg/L), $CuSO_4$ (1 mg/L), and NaClO (3 mg/L) each achieved over 73% mortality of *L. fortunei*. Enzymatic activity analysis revealed distinct response patterns. NS caused sustained increases in superoxide dismutase (SOD) and glutathione-S-transferase (GST), malondialdehyde (MDA) increased significantly at 70% mortality, succinate dehydrogenase (SDH) were all below the control group, while acetylcholinesterase (AChE) slightly increased and then decreased. $CuSO_4$ induced continuous SOD increase, fluctuated MDA and GST levels, similar inhibition of SDH to NS, elevated AChE at 50% mortality. NaClO resulted in moderate SOD increase, severe MDA accumulation, an initially GST increase and then decrease, elevated SDH at 70% mortality, and higher AChE at 50% mortality. These results suggest that NS and $CuSO_4$ suppress the physiological activity of *L. fortunei* primarily through oxidative stress and mitochondrial inhibition, whereas NaClO acts directly via membrane damage and oxidative injury at late stage. Histological examination of gills and gonads at 50% and 70% mortality revealed that NS triggered gill structural abnormalities and gonad atroph, $CuSO_4$ caused gill atrophy and gonad cavitation, NaClO induced only minor changes at 50% mortality but major gill cell loss and gonad nuclear disappearance at 70% mortality. The results of HE showed that all three chemical agents caused structural disorder of the gill filaments, gonadal atrophy and cavitation, and even disappearance of nuclei in *L.fortunei*, leading to significant tissue damage. These findings provide theoretical basis for selecting effective chemical controls including NS, $CuSO_4$ and NaClO against *L. fortunei* in hydraulic and enclosed infrastructure.

Key words: *Limnoperna fortunei*; chemical agents; enzymatic activity; hematoxylin-eosin (HE) staining

CLC number: X592

Received date: 2025-07-15

Biography: LIU Jian, male, Master candidate, research direction: prevention and control of biological fouling in water conservancy projects. E-mail:liujian649@163.com

† Corresponding author. E-mail: litiancui@cjjg.mee.gov.cn

0 Introduction

Limnoperna fortunei (*L. fortunei*), indigenous to southern China[1], has become a globally invasive freshwater bivalve through anthropogenic spread—chiefly via maritime transport. Since its introduction, it has established dominant populations in Brazil, Argentina[2], Japan, and South Korea[3], driven by exceptional post-invasion dispersal capabilities.

Adult *L. fortunei* release vast quantities of larvae, transported efficiently by water currents to colonise substrates including metal, concrete, and rock[4]. These larvae metamorphose into juveniles within days, secreting abundant byssal threads to anchor securely. A defining trait is its aggregative growth: mussels form dense, interwoven clusters at attachment points through mutual byssal entanglement[5]. Aggregated colonies exhibit stronger adhesion than solitary individuals, with sessile assemblages creating persistent biofouling matrices.

This invasive strategy coupled with rapid larval dispersal and year-round reproduction, enables *L. fortunei* to colonise freshwater systems aggressively. Dense aggregations pose ecological and economic risks, particularly in engineered infrastructure like power plant intakes[5].

The ecological and economic impacts of *L. fortunei* invasion primarily involve four aspects: 1) Corrosive effects on concrete and metal surfaces damage hydraulic infrastructure[6]. 2) High-density colonisation in water pipelines increases wall roughness coefficients, reduces flow cross-section, and decreases conveyance efficiency[7]. 3) Massive aggregations in pipelines and power station filters cause blockages, leading to equipment shutdowns, safety hazards, and economic losses[8]. 4) Population mass mortality result in elevated ammonia-nitrogen or organic matter concentrations[9], altered microbial communities[10], viral pathogen introduction[11], and toxic gas emissions[12].

Control strategies for *L. fortunei* primarily involve physical, chemical, and biological methods[13]. Physical approaches include the application of anti-fouling coatings[14], thermal treatment[15], hypoxic sealing[16], ultrasonic disruption, and manual or robotic removal[17]. Chemical methods typically utilize oxidizing agents such as sodium hypochlorite, chloramine, potassium permanganate, and hydrogen peroxide[18], or copper sulfate ($CuSO_4$) and glyphosate[19] to disrupt the structures of byssal threads and induce detachment[20]. Biological control involves the introduction of competitor or predator fish species. This involves releasing species with similar filter-feeding habits to compete for food, or alternatively, deploying piscivorous fish that actively prey on *L. fortunei*[21-22]. Practical implementations often combine multiple technologies, tailored to specific infrastructure and environmental contexts to achieve effective population management.

In comparison with other control methods, chemical treatment provides the most rapid efficacy and relatively low cost, rendering it the favoured emergency-response option for most water conservancy projects. Current research mainly focuses on molluscicidal efficacy[23] and byssus disruption mechanisms[24] of chemical agents. However, there are limited investigations into other compound types, including flocculants, insecticides, and composite formulations. To fill this research gap, this study compared experimentally the molluscicidal effects of eight common chemicals copper sulfate ($CuSO_4$), chloramine, sodium hypochlorite (NaClO), salicylic acid, glyphosate, chitosan-based flocculant, nicotinoyl aniline sulfate (NS), and polyquaternium on *L. fortunei*. We chose three highly effective agents to measure oxidative stress biomarkers, namely superoxide dismutase (SOD)[25], glutathione S-transferase (GST)[26] and malondialdehyde (MDA)[27], meanwhile, acetylcholinesterase (AChE)[28] was detected to assess the neurotoxicity of chemical agents on *L. fortunei*. The activity of succinate dehydrogenase (SDH)[29] was analyzed to evaluate the disruption of the respiratory pathway. Histological analysis of gill and gonad tissues using hematoxylin-eosin (HE) staining was conducted at different mortality stages to characterize pathological damage. This research contributes to the optimization of chemical agent selection and offers mechanistic insights into *L. fortunei* control.

1 Materials and Methods

1.1 Experimental Materials

L. fortunei specimens were collected from a pontoon boat at the confluence of the Hanjiang and the Yangtze River (30°27'0" N, 114°13'0" E). Concurrently, the water was collected from the adjacent locations (n= 3) to characterize baseline conditions. Following transport to the laboratory, viable individuals were selected and acclimatized in a recirculating system (100 L capacity) containing filtered site-sourced water (0.45 μm mesh). Custom glass tanks sized 30 cm (length) × 18 cm

(width) × 20 cm (height) were prepared, and in situ raw water was collected during *L. fortunei* sampling, with 10 L of it then added to each tank for the experiment.

A triple-function aeration pump (36V AC, rated flow of 1 000 L/h) was installed in the glass tank to provide oxygenation, water circulation, and mechanical filtration. Before introducing *L. fortunei*, the height of the aeration pump and the intake valves were adjusted to maintain a uniform flow velocity of 0.05-0.10 m/s and a gas flow rate of 2-3 L/min. At the same time, a thermometer and a thermostatic device were inserted into the tank to ensure that the water temperature is between 19 and 22 ℃. The quality of in situ water used in the experiment is shown in Table 1.

Table 1 Water quality criteria for site-sourced water used in *L. fortunei* experiments

Physicochemical indicators	Value
Water temperature/℃	19-22
Dissolved oxygen/mg·L^{-1}	7.0-9.0
pH	7.6-8.4
Conductivity /μS·cm^{-1}	300-400
Permanganate index /mg·L^{-1}	1.2-2.8
Total nitrogen /mg·L^{-1}	1.8-2.6
Nitrate nitrogen /mg·L^{-1}	1.5-2.0
Ammonia nitrogen /mg·L^{-1}	0.02-0.08
Nitrite nitrogen /mg·L^{-1}	0.002-0.009
Total phosphorus /mg·L^{-1}	<0.1
Suspended solids /mg·L^{-1}	<10
Chlorophyll-a /μg·L^{-1}	3-8

1.2 Experimental Design

Healthy *L. fortunei* individuals (uniform body length: 15-20 mm) were selected and acclimatised in the experimental apparatus for 3 days. During this period, dead specimens were removed daily and replaced with viable individuals to ensure pre-experimental (24 h prior to chemical dosing) mortality remained less than 2%.

For each chemical agent, 15 glass tanks (20 qualified *L. fortunei* individuals in each glass tank) were allocated to 5 parallel groups: 1 blank control (no chemical) and 4 treatment groups (graded concentrations). The concentration gradients of the eight chemicals are as follows: $CuSO_4$ at 0.5, 1.0, 3.0, and 5.0 mg/L; chloramine, salicylic acid, chitosan-based flocculant, and NaClO all at 1.0, 3.0, 5.0, and 10.0 mg/L; glyphosate at 0.1, 0.3, 0.5, and 1.0 mg/L; NS at 1.0, 2.0, 3.0, and 5.0 mg/L; and polyquaternary ammonium salt at 10.0, 30.0, 50.0, and 100.0 mg/L. These concentration gradients were designed to facilitate dose-response analyses. Concentrations were primarily determined based on preliminary experiments (n =3, 96 h acute toxicity tests) and literature-derived effective doses[18, 20]). High-concentration stock solutions were freshly prepared and delivered via a peristaltic pump (Watson-Marlow 323S) to achieve target concentrations, with dosing valves adjusted to ensure uniform injection over 1 h (± 5 min precision).

1.3 Indicators and Analysis

1.3.1 Mortality rate

Molluscicidal efficacy was quantified using mortality rate, calculated as:

$$R = \frac{N_s}{N} \times 100\%,$$

where: R, mortality rate, %; N_s, number of deceased *L. fortunei* individuals; N, total number of experimental mussels at the onset of exposure.

1.3.2 Enzyme activity test

After experiments with eight chemical agents, the three most effective agents and their corresponding concentrations were selected for enzyme activity assays in *L. fortunei*. The collection, acclimatization, experimental setup, and procedures for *L. fortunei* remained consistent with those previously described. Mortality rates were recorded at 12 h intervals in each experimental group, and any deceased individuals were promptly removed. In the control group, healthy *L. fortunei* specimens were dissected at the start of exposure. In the treatment groups, three *L. fortunei* were randomly selected for dissection when the relative mortalities reached 20%, 50%, and 70%, respectively. After dissection, internal organs were collected and stored at −80 ℃. Immediately after sacrifice, the activities or contents of SOD, MDA, GST, SDH, and AChE were determined.

Specific analytical methods are as follows:

SOD: Precisely weighed tissue samples (0.1-0.3 g, Sartorius Cubis Pro balance, ± 0.1 mg precision) were transferred to 3 mL centrifuge tubes. Normal saline was added at a 1∶9 ratio (tissue weight/g∶ saline volume/mL), and samples were homogenised using a low-temperature homogeniser (4 ℃, IKA T10 basic) for 3 cycles of 30 s each. Homogenates were centrifuged at 2 500-4 000 r/min (1 200-2 500 ×*g*, Eppendorf 5810R, 4 ℃) for 10 min, and supernatants (10% homogenates) were collected for analysis.

Prior to assays, preliminary experiments determined the optimal dilution factor: a 5-fold dilution of

10% homogenate with normal saline (to a final concentration of 2%) minimized matrix interference. All assays followed kit protocols (Nanjing Jiancheng A001-3, A003-1), with absorbance measured at 450 nm using a microplate reader (Tecan Infinite M200 Pro).

Calculation formula is as follows:

$$I_{\mathrm{SOD}}=\frac{\left(A_c-A_{\mathrm{cb}}\right)-\left(A_t-A_{\mathrm{tb}}\right)}{\left(A_c-A_{\mathrm{cb}}\right)},$$

$$\mathrm{EA}_{\mathrm{SOD}}=I_{\mathrm{SOD}}\div 50\%\times \mathrm{DF}\div C_p,$$

where: I_{SOD}, SOD inhibition rate, %; A, absorbance values of different groups, c, control, cb, control blank, t, test, tb, test blank; $\mathrm{EA}_{\mathrm{SOD}}$, relative SOD activity, U/mgprot; DF, dilution factor of the assay system; C_p, protein concentration of sample homogenate, mgprot/mL.

MDA: Tissue samples underwent the same pretreatment as detailed above. After preparing 10% homogenates (tissue: normal saline, 1 ∶ 9 w/v), absorbance was measured at 532 nm using a microplate reader following kit protocols for reagent addition and incubation.

The MDA calculation formula is:

$$C_{\mathrm{MDA}}=\frac{A_t-A_c}{A_s-A_b}\times C_s\div C_p,$$

where: C_{MDA}, MDA concentration, nmol/mgprot; A, absorbance values of different groups, s, standard, b, blank; C_s, standard concentration, 10 nmol/mL.

GST: Tissue samples underwent the same pretreatment as described. After preparing 10% homogenates (tissue: normal saline, 1 ∶ 9 w/v), preliminary experiments using the same microplate reader determined the optimal dilution: a 5-fold dilution of 10% homogenate to 2% final concentration minimised assay interference. Subsequent steps followed the enzyme activity kit protocol, with absorbance measured at 412 nm. The calculation formula is as follows:

$$\mathrm{EA}_{\mathrm{GST}}=\frac{A_c-A_t}{A_s-A_b}\times C_s\times \mathrm{DF}\div T\div(V\times C_p),$$

where: $\mathrm{EA}_{\mathrm{GST}}$, GST activity, U/mgprot; C_s, 20 nmol/L; T, enzymatic reaction time, 30 min.

AChE: Tissue samples were pretreated as described. After preparing 10% homogenates (tissue: normal saline, 1 ∶ 9 w/v), all steps followed the enzyme assay kit protocol. Absorbance was measured at 412 nm with a microplate reader. Calculation formula is as follows:

$$\mathrm{EA}_{\mathrm{AChE}}=\frac{A_t-A_c}{A_s-A_b}\times C_s\div C_p,$$

where: $\mathrm{EA}_{\mathrm{AChE}}$, AChE activity, U/mgprot; C_s, 1 nmol/L.

SDH: Tissue samples were pretreated as described. After preparing 10% homogenates (tissue: normal saline, 1 ∶ 9 w/v), all steps followed the enzyme assay kit protocol. Absorbance was measured at 600 nm with a spectrophotometer at 10 s and 70 s after initiation of the reaction. For each sample, ΔA ($A_{70\,\mathrm{s}}-A_{10\,\mathrm{s}}$) was recorded. Calculation formula is as follows:

$$\mathrm{EA}_{\mathrm{SDH}}=\frac{A_1-A_2}{T}\div U\div(V\times C_p),$$

where: $\mathrm{EA}_{\mathrm{SDH}}$, SDH activity, U/mgprot; A_1, absorbance at 10 s; A_2, absorbance at 70 s; U, unit defined as a 0.01 decrease in absorbance per unit time.

Protein Concentration: Protein concentration (C_p) was measured concurrently with enzyme assays using identically pretreated samples: tissues were homogenized to 10% (tissue: normal saline, 1 ∶ 9 w/v), diluted 10-fold to 1% homogenate, and processed following the kit protocol before absorbance was measured at 562 nm with a microplate reader.

$$C_p=\frac{A_t-A_b}{A_s-A_b}\times C_s\times \mathrm{DF},$$

where: C_p, protein concentration, μgprot/mL; C_s, 524 μg/mL.

1.3.3 HE analysis

L. fortunei gill and gonad tissues from 50% and 70% mortality groups of the three agents were processed for histological analysis. The detailed procedures were as follows: 1) Sample excision: Tissues were dissected intact from treated mussels. 2) Fixation & washing: Fixed in 4 % paraformaldehyde for 24 h, rinsed with 70% ethanol to remove fixative. 3) Gradient dehydration: Sequential ethanol incubation: 70% ethanol for 4 h; 80% ethanol for 2×2 h; 95% ethanol for 2×45 min; 100% ethanol for 2×45 min. 4) Clearing & embedding: Treated with xylene, embedded longitudinally in paraffin. 5) Sectioning: 5 μm longitudinal sections cut using a microtome (Leica RM2235). 6) HE staining: Hematoxylin (nuclear) and eosin (cytoplasmic) staining, mounted with DPX resin. 7) Imaging: Visualized at ×10-×40 magnification (Olympus BX53), and representative fields photographed.

2 Results

2.1 Experimental Results of Chemical Agent Treatment

Mortality of *L. fortunei* exposed to eight chemical agents is presented in Fig. 1. As bivalves, *L. fortunei* initially closed shells in response to chemical stress[30], but prolonged exposure (≥48 h) exceeded tolerance thresholds,

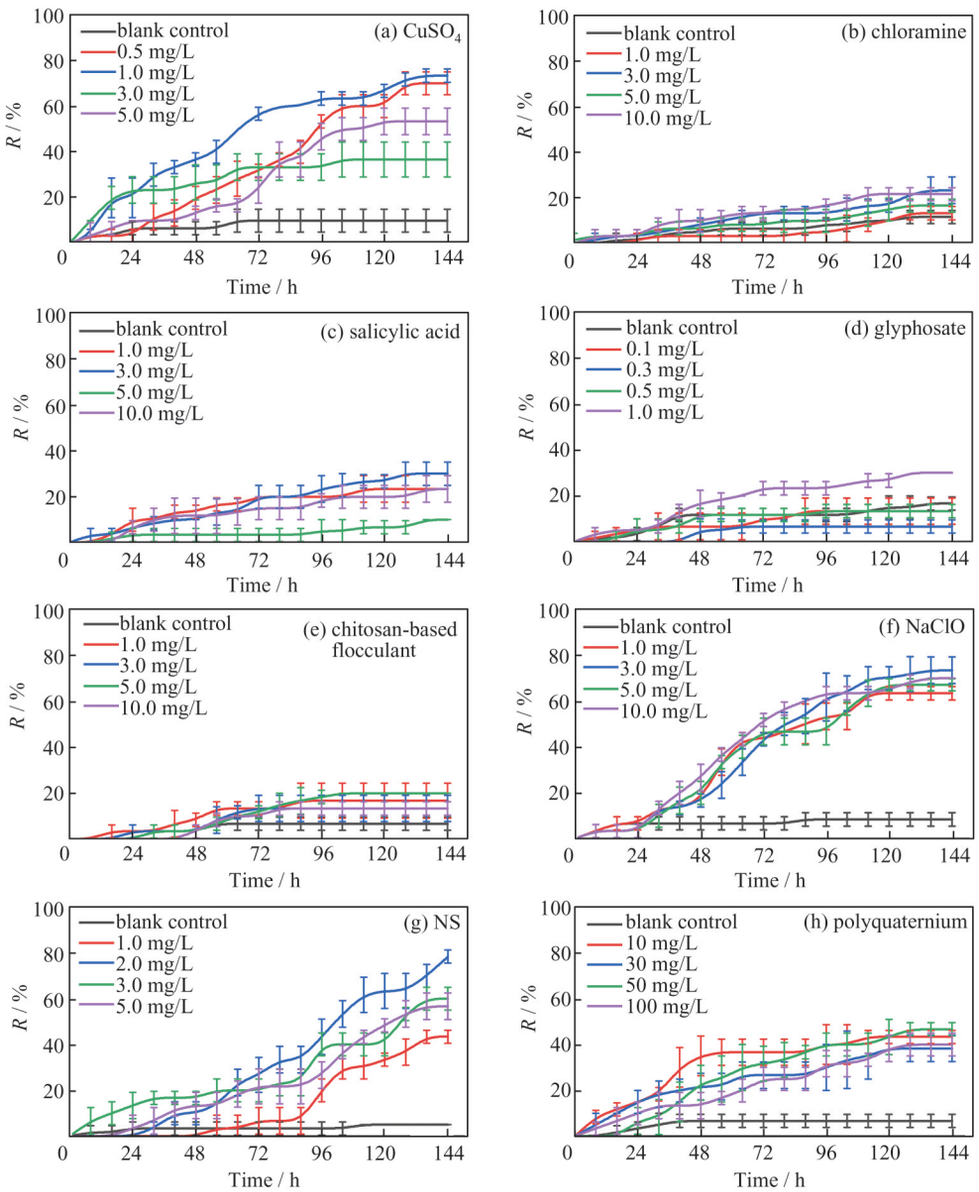

Fig. 1 144 h mortality changes of *L. fortunei* treated with eight chemical agents

triggering shell re-opening. This allowed agents to diffuse into tissues via inhalant siphons, initiating cytotoxic damage.

Exposure of *L. fortunei* to $CuSO_4$ exhibited a concentration-dependent biphasic response: molluscicidal efficacy peaked at 1.0 mg/L (73.3% mortality at 144 h, representing a 63.3 percentage points increase over the control), declining at higher doses. This optimal efficacy aligned with Cu^{2+}-induced oxidative stress[30], where excess ions disrupt antioxidant homeostasis—generating reactive oxygen species (ROS) that peroxidise membrane unsaturated fatty acids, leading to cellular damage[31].

When treating *L. fortunei* with chloramine, mortality showed minimal concentration dependence: the maximum 23.3% mortality at 3.0 mg/L represented a 11.7 percentage points increase over the control. Previous research highlighted stronger molluscicidal efficacy at 25 ℃ vs. 20 ℃, but required prolonged exposure[32] —posing challenges for water conservancy projects where sustained chemical dosing is operationally infeasible, and generator shutdowns for treatment incur significant power generation losses. Therefore, chloramines are not suitable for the prevention and control of freshwater mussels.

Salicylic acid is a polyphenolic compound ubiquitous in organisms that interacts with lecithin membranes at physiological concentrations, altering membrane mechanics and perturbing cellular transport and enzymatic activities[33]. When tested on *L. fortunei*, salicylic acid in-

duced moderate mortality: the 3.0 mg/L optimal group achieved a 30 percentage points increase over the control, significantly lower than $CuSO_4$ or NaClO.

Glyphosate exposure induced no significant mortality differences compared with the control group. Studies report 0-20 mg/L glyphosate minimally affects *L. fortunei* shell-opening rates, with low concentrations showing negligible molluscicidal activity while mussels maintain active filter-feeding[34-35]. This limited efficacy may arise from glyphosate's short aquatic half-life[36] and surface biofilms on *L. fortunei* that adsorb/degrade the herbicide: Gammaproteobacteria isolated from mussel surfaces degrade glyphosate post-exposure[37]. While low-dose glyphosate is ineffective against *L. fortunei*, effective concentrations can pose environmental risks[35], especially in water conservancy projects that must adhere to strict water quality standards.

Chitosan, a natural, environmentally friendly polymeric flocculant[38], acts by clarifying water and forms a gelatinous biofilm on *L. fortunei* surfaces, impeding respiratory and material exchange. However, this study revealed limited molluscicidal efficacy: increasing the concentrations from 1.0 mg/L to 5.0 mg/L resulted in only a 14.23 percentage points increase, suggesting that its potential for water treatment outweighs that for direct mollusc control.

Sodium hypochlorite (NaClO) is the most widely used chemical molluscicide for *L. fortunei*, exhibiting potent molluscicidal activity[39] and dissolving byssal threads[40]. In this study, all NaClO concentrations significantly increased mortality: 1.0 mg/L (55 percentage points increase over the control), 3.0 mg/L (65 percentage points increase over the control), 5.0 mg/L (56.67 percentage points increase over the control), and 10 mg/L (61.67 percentage points increase over the control), with the 3.0 mg/L dose showing optimal efficacy.

NS, a non-toxic aquaculture water modifier, selectively eliminates mollusks (including *L. fortunei*) while remaining non-lethal to fish and shrimp. This study found 2.0 mg/L NS induced 78.33% *L. fortunei* mortality (73.33 percentage points increase over the control), demonstrating potent and species-specific molluscicidal activity.

As a cationic polymer, polyquaternium acts by binding to negatively charged components in *L. fortunei* biofilms. These biofilms form vital extracellular matrices that facilitate respiration and feeding. Disruption of these biofilms by polyquaternium impairs gas exchange and material transport, leading to mortality. In this study, 3.0 mg/L polyquaternium induced a 40 percentage points increase over the control, aligning with its biofilm-targeted mechanism.

Mortality analysis identified three optimal agents: NS (2.0 mg/L), $CuSO_4$ (1.0 mg/L), and NaClO (3.0 mg/L). These chemicals exhibited potent molluscicidal activity at lower concentrations than other tested compounds. NS achieving 78.3% mortality, $CuSO_4$ 73.3%, and NaClO 65%, making them more suitable for *L. fortunei* control in water conservancy projects due to reduced operational doses and environmental risks.

2.2 Results of Enzyme Activity Test Experimental

To investigate the molluscicidal mechanisms of NS (2.0 mg/L), $CuSO_4$ (1.0 mg/L) and NaClO (3.0 mg/L) against *L. fortunei*, we determined enzyme activities and conducted histological analyzes on tissues from mussels sampled before treatment and post-treatment mortality rates of 20%, 50% and 70%. Enzymatic activities (SOD, MDA, GST, SDH, AChE) and protein content were measured in selected tissues. Results are presented as mean ± SD, with statistical significance (unpaired *t*-test,**P*<0.05, ***P*<0.01, ****P*<0.001) determined by Student's *t*-test against the control. Enzymatic data are visualized in Table 2.

2.2.1 Enzymatic activity of *L. fortunei* after NS treatment

Exposure to NS led to significant elevations in the activities of SOD and GST in *L. fortunei*. Meanwhile, the levels of MDA initially increased and subsequently decreased, and the activity of SDH decreased at first, then partially recovered but remained consistently lower than that of the control group.

There was a positive correlation between SOD activity and the progression of mortality. In the control group, the SOD activity was (9.187 3 ± 0.757 5) U/mgprot. It increased to (11.688 7 ± 1.061 7) U/mgprot at a 20% mortality level (P<0.05), to (11.549 8 ± 0.931 7) U/mgprot at a 50% mortality level (P<0.05), and sharply rose to (15.360 9 ± 1.344 7) U/mgprot at a 70% mortality level (P<0.01).

MDA tracking SOD dynamics but at reduced amplitude (e. g., 70% mortality: SOD +67% vs. MDA +22% over the control). The MDA levels increased from (8.687 3 ± 0.828 0) nmol/mgprot at a 20% mortality level to (10.566 0 ± 2.039 3) nmol/mgprot at a 70% mortality level, both of which were significantly higher than that of the control group (P<0.05).

Table 2 Enzymatic activities in the tissues of *L. fortunei* after chemical agent treatments

Treatment		SOD/ (U·mgprot^{-1})	MDA/(nmol· mgprot^{-1})	GST/ (U·mgprot^{-1})	SDH/ (U·mgprot^{-1})	AChE/ (U·mgprot^{-1})
Control		9.187 3±0.757 5	7.275 3±1.118 7	1.453 7±0.154 9	6.660 8±0.682 5	0.126 6±0.011 0
A	*R*=20%	11.688 7±1.061 7*	8.687 3±0.828 1*	2.668 9±0.558 0*	1.800 7±0.139 6***	0.130 3±0.014 2
	R=50%	11.549 8±0.931 7*	7.808 0±0.590 3	11.474 4±1.266 3***	0.508 9±0.203 7***	0.082 2±0.011 4**
	R=70%	15.360 9±1.344 7**	10.566 0±2.039 3*	15.681 0±0.925 5***	3.837 0±0.331 4**	0.112 7±0.019 1
B	*R*=20%	11.755 7±1.033 6*	34.496 1±3.528 6***	7.811 8±0.644 0***	1.481 7±0.128 1***	0.126 1±0.011 3
	R=50%	11.247 1±1.233 3*	12.348 7±1.990 2**	5.717 6±0.793 5***	1.185 2±0.211 1***	0.185 4±0.013 0**
	R=70%	12.116 1±1.120 6*	19.338 2±1.381 8***	7.672 8±0.114 6***	3.658 9±0.571 9**	0.126 1±0.010 0
C	*R*=20%	8.450 0±0.546 2	6.605 4±1.595 6	3.678 4±0.681 8**	1.975 6±0.568 2***	0.094 2±0.011 3*
	R=50%	9.378 0±0.883 7	4.728 2±0.564 8*	6.131 5±0.272 1***	1.256 7±0.240 5***	0.263 4±0.015 7***
	R=70%	11.665 4±1.128 7*	26.277 9±2.12 1***	4.652 3±0.120 0***	10.078 5±0.815 6**	0.167 1±0.007 0**

A=NS, B=$CuSO_4$, C=NaClO. Data are expressed as mean ± SD (n=3). Multiple comparisons (9 pairs: 3 agents × 3 mortality levels vs. control) were corrected using Bonferroni method (corrected α = 0.005 6). * indicates P<0.05, ** indicates P<0.01, *** indicates P<0.001.

GST activity increased dramatically with rising mortality. It was (2.67 ± 0.56) U/mgprot at 20% mortality, (11.47 ± 1.27) U/mgprot at 50% mortality, and (15.68 ± 0.93) U/mgprot at 70% mortality. All values were extremely significantly higher than that of the control group ((1.45 ± 0.15) U/mgprot, P<0.001).

SDH activity first decreased sharply and then partially recovered with increasing mortality, but all values remained significantly lower than the control (P<0.05). It dropped to (1.80 ± 0.14) U/mgprot and (0.51 ± 0.20) U/mgprot at 20% and 50% mortality, rebounding to (3.84 ± 0.33) U/mgprot at 70% mortality.

AChE exhibited minimal fluctuations, except for a significant decrease (−34.92% vs the control) observed at a 50% mortality level (P<0.05).

2.2.2 Enzymatic activity of *L. fortunei* after $CuSO_4$ treatment

$CuSO_4$ exposure induced mild SOD elevation, pronounced increase of GST, marked MDA fluctuations (initial surge followed by decline), and incomplete recovery of suppressed SDH activity in *L. fortunei* tissues. AChE increased significantly only at 50% mortality.

SOD showed elevation across mortality levels: (11.76 ± 1.03) U/mgprot at a 20% mortality level, (11.25 ± 1.23) U/mgprot at a 50% mortality level, and (12.12 ± 1.12) U/mgprot at a 70% mortality level—all exceeding the control ((9.19 ± 0.76) U/mgprot, P<0.05).

MDA exhibited a biphasic response: a 3.74-fold surge to (34.50 ± 3.53) nmol/mgprot at 20% mortality (P< 0.001), followed by a 64% decline to (12.35 ± 1.99) nmol/mgprot at 20% mortality (P<0.01), and a rebound to (19.34 ± 1.38) nmol/mgprot at 70% mortality (P<0.001).

GST activity was significantly higher than that in the control group (all P<0.001), reaching (7.81 ± 0.64) U/mgprot at 20% mortality and (7.67 ± 0.11) U/mgprot at 70% mortality, and slightly lower at 50% mortality (5.72 ± 0.79) U/mgprot.

SDH activity decreased sharply and then partially recovered, but remained below the control level at all mortality levels. It dropped to (1.48 ±0.13) U/mgprot and (1.19 ± 0.21) U/mgprot at 20% and 50% mortality, respectively (P<0.001), and then rebounded to (3.66 ± 0.57) U/mgprot at 70% mortality.

AChE activity peaked only at 50% mortality, reaching (0.185 ± 0.013) U/mgprot (P<0.01), while at other mortality levels it showed no significant difference from the control (P>0.05).

2.2.3 Enzymatic activity of *L. fortunei* after NaClO treatment

NaClO exposure elicited divergent enzymatic responses in *L. fortunei*: mild SOD elevation, biphasic GST dynamics, transient MDA/SDH suppression with late recovery, and AChE activation at 50% mortality.

SOD showed incremental increases: (8.45 ± 0.55) U/mgprot at 20% mortality, (9.38 ± 0.88) U/mgprot at 50% mortality, and (11.67 ± 1.13) U/mgprot at 70% mortality—only the 70% mortality group differing significantly from the control ((9.19 ± 0.76) U/mgprot, P<0.05).

MDA exhibited a U-shaped trajectory: non-significant decline at 20% mortality (P>0.05), significant drop to (4.73 ± 0.56) nmol/mgprot at 50% mortality (P<0.05), followed by a surge to (26.28 ± 2.12) nmol/mgprot at 70% mortality (P<0.01).

GST peaked at 50% mortality ((6.13 ± 0.27) U/mgprot, P<0.001) before declining to (4.65 ± 0.12) U/mgprot at 70% mortality—both exceeding the control ((1.45 ± 0.15) U/mgprot, P<0.001).

SDH mirrored NS/$CuSO_4$ patterns: early suppression to (1.98 ± 0.57) U/mgprot at 20% mortality and (1.26 ± 0.24) U/mgprot at 50% mortality, followed by robust recovery to (10.08 ± 0.82) U/mgprot at 70% mortality—uniquely surpassing the control ((6.66 ± 0.68) U/mgprot, P<0.01).

AChE displayed mortality-phase specificity: suppression at 20% mortality ((0.094 ± 0.011) U/mgprot, P< 0.05), hyperactivation at 50% mortality ((0.263 ± 0.016) U/mgprot, P<0.01), and moderate elevation at 70% mortality ((0.167 ± 0.007) U/mgprot, P<0.01).

2.3 HE Staining

HE-stained gill filament and gonad sections from *L. fortunei* are presented in Figs. 2-5. Control (untreated) gill filaments (Fig. 2(a)) showed regular epithelial architecture with bilaterally symmetric lateral cilia, intact spindle-shaped nuclei, and ordered cell alignment. Control gonads (Fig. 2(b)) exhibited intact glandular parenchyma with abundant irregular epithelial cells containing rounded, basophilic nuclei and eosinophilic cytoplasm.

Treatment groups (Figs. 3-5) are staged by mortality: gill filaments at 50% mortality (Fig. 3(a), 4(a), 5(a)) and 70% mortality (Fig. 3(c), 4(c), 5(c)); gonads at 50% mortality (Fig. 3(b), 4(b), 5(b)) and 70% mortality (Fig. 3(d), 4(d), 5(d)).

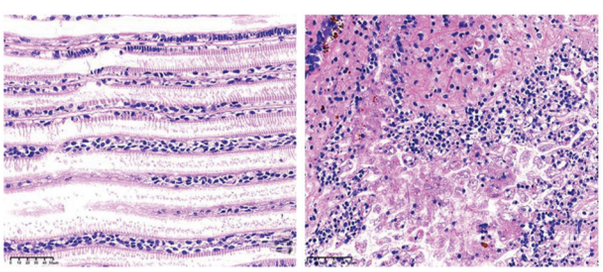

Fig. 2 HE-stained sections of gill filaments (a) and gonads (b) in control *L. fortunei*

2.3.1 Result of HE staining after NS treatment

NS-induced histological lesions in *L. fortunei* gill filaments and gonads (Fig. 3) are described below:

At 50% mortality (Fig. 3(a)): There was irregular inter-filament spacing compared with the control. There was also focal lateral cilia loss (D_1) and nuclear malformation accompanied by chromatin dispersion (D_2). The decrease in mid-filament cell density was accompanied by a corresponding increase in apical cellular aggregation, suggesting a compensatory response to epithelial injury.

At 70% mortality (Fig. 3(c)): Severe atrophy was observed, accompanied by near-total loss of cilia and depletion of cells across the filaments. The presence of nuclear pyknosis and karyorrhexis confirmed that the damage was irreversible (D_3).

At 50% mortality (Fig. 3(b)): Mild glandular atrophy was observed (D_4). There was nuclear dispersion (D_5), along with vacuolation and a honeycombed parenchymal architecture (D_6).

At 70% mortality (Fig. 3(d)): Advanced atrophy with cavitation was present, resulting in loss of parenchyma. The cellular architecture was disorganized, and there was chromatin condensation.

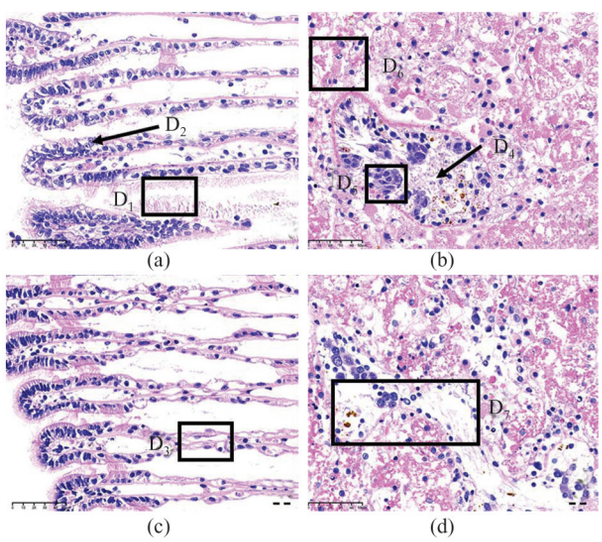

Fig. 3 Gill filaments of *L. fortunei* treated with NS (a, c: 50% and 70% mortality) and gonads (b, d: 50% and 70% mortality)

2.3.2 Result of HE staining after $CuSO_4$ treatment

$CuSO_4$-induced histological lesions in *L. fortunei* gills/gonads (Fig. 4) surpassed NS-induced damage, reflecting Cu^{2+}-mediated membrane peroxidation, as described below:

At 50% mortality (Fig. 4(a)): Severe atrophy was observed. The inter-filament gaps were widened compared to the control. Mid-filament vacuolation (D_1) was present. Nuclear deformation (D_2) accompanied by chromatin dispersion indicated early apoptotic signaling.

At 70% mortality (Fig. 4(c)): The epithelium was fragmented (D_3), with scattered nuclear remnants showing karyorrhexis (D_4), and there was near-total cilia loss.

At 50% mortality (Fig. 4(b)): Atrophic pink connective tissue was seen. Nuclear malformations (D_5) and vacuolation (D_6) were present.

At 70% mortality (Fig. 4(d)): Advanced cavitation was present, resulting in loss of parenchyma (D_7), and there was chromatin dispersion (D_8). This damage exceeded the NS-induced damage, likely due to Cu^{2+}-induced irreversible lipid peroxidation.

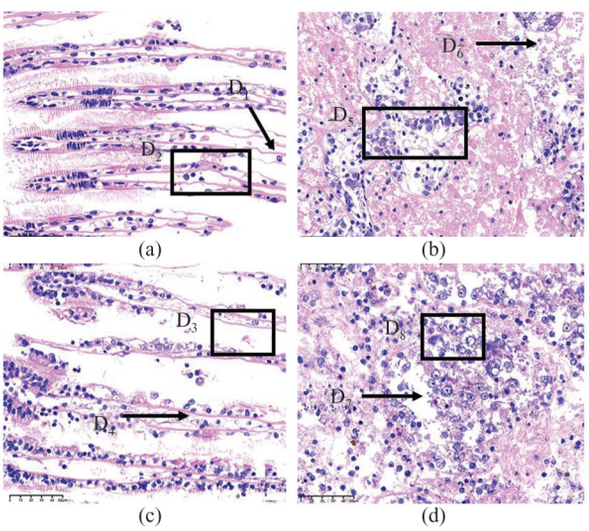

Fig. 4 Gill filaments of *L. fortunei* treated with $CuSO_4$ (a, c: 50% and 70% mortality) and gonads (b, d: 50% and 70% mortality)

2.3.3 Result of HE staining after NaClO treatment

NaClO-induced histological lesions in *L. fortunei* gills/gonads (Fig. 5) exhibited a distinct toxicity pattern, as described below:

At 50% mortality (Fig. 5(a)): There was mild mid-filament cell depletion compared to the control and focal chromatin dispersion (D_1). However, lateral cilia and epithelial architecture were preserved, which was consistent with closed-shell protection.

At 70% mortality (Fig. 5(c)): Apical cellular aggregation, a compensatory response, was observed. There was lateral cilia loss (D_2) and mid-filament cavitation was also present (D_3). Irregularly shaped circular vacuoles (D_4) were observed, which were distinct from the random cavitation patterns seen in other treatments.

At 50% mortality (Fig. 5(b)): Sparse nuclear malformation and chromatin dispersion were seen (D_5). Occasional amber vitellin deposits (L_1) indicated early reproductive disruption, yet nuclear integrity remained largely intact.

At 70% mortality (Fig. 5(d)): Advanced atrophy with connective tissue cavitation was present (D_6). Nuclear deformation (D_7) was also observed.

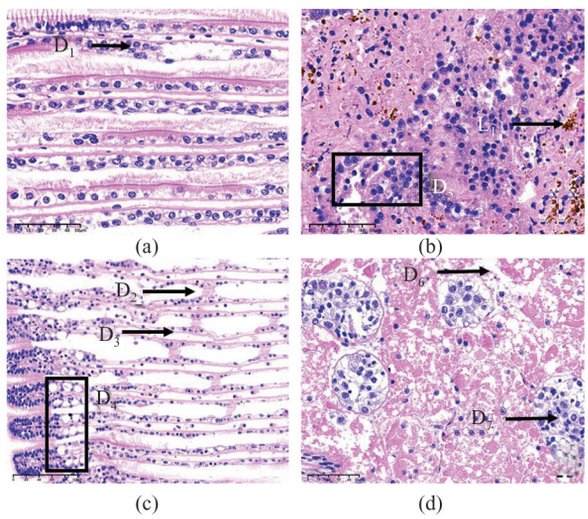

Fig. 5 HE-stained gill filaments (a, c: 50% and 70% mortality) and gonads (b, d: 50% and 70% mortality) of *L. fortunei* treated with NaClO

3 Discussion

3.1 Oxidative Stress Defense and Toxicity Mechanisms in Aquatic Mollusks

Aquatic mollusks deploy antioxidant enzymes and non-enzymatic systems to counteract oxidative stress[41]. As the first-line antioxidant defense, SOD catalyzes superoxide radicals (O_2^-) and protons (H^+) into oxygen (O_2) and hydrogen peroxide (H_2O_2)[42], which is subsequently reduced to water by glutathione peroxidase (GPx). GST works in tandem with GPx to scavenge reactive oxygen species (ROS) and organic peroxides, safeguarding cellular membranes from oxidative damage[43].

MDA, a biomarker of lipid peroxidation, arises from polyunsaturated fatty acid oxidation in membranes and directly reflects oxidative injury severity[44]. Meanwhile, SDH is a mitochondrial enzyme that links oxidative phosphorylation to electron transport. It supplies electrons to the aerobic respiratory chain in mollusk cells, a function particularly critical for energy-intensive processes such as shell maintenance[45].

Upon chemical challenge, *L. fortunei* initially seals its shell to limit material exchange, but prolonged oxidative stress depletes energy stores, compelling shell reopening and resumed aerobic respiration beyond a critical closure duration[32]. AChE is an enzyme that hydrolyzes acetylcholine to modulate muscle contraction and neuro-

transmission[46]. It exhibits dual toxicity thresholds: inhibition greater than or equal to 20% indicates chemical insult, whereas inhibition greater than or equal to 50% endangers survival[47]. Paradoxically, hyperactivation (e.g., 50% mortality in NaClO-treated mussels) disrupts neuromuscular coordination, leading to debilitating muscle weakness[48].

3.2 NS-Induced Responses

NS exposure elicited coordinated SOD-MDA elevation in *L. fortunei*, with MDA tracking SOD dynamics but at reduced amplitude. As mortality increased from 20% to 50%, GST activity rose 4.87-fold (from (2.67 ± 0.56) U/mgprot to (15.68 ± 0.93) U/mgprot), while SDH activity fell to a nadir of (0.51 ± 0.20) U/mgprot. This inverse relationship marked the onset of mitochondrial dysfunction. Histological evidence of cellular/nuclear damage indicated NS-induced oxidative stress remained within reparable limits, partially buffered by SOD/GST upregulation. However, prolonged exposure (≥50% mortality) exacerbated injury: AChE suppression mirrored organophosphorus pesticide neurotoxicity[49], disrupting cholinergic signaling. Collectively, NS exerts molluscicidal effects via dual pathways: oxidative stress overwhelming antioxidant defenses, compounded by mitochondrial energy crisis and neurotransmission impairment.

3.3 $CuSO_4$-Induced Responses

$CuSO_4$ exposure induced modest yet significant SOD elevation in *L. fortunei*, which aligned with prior reports of Cu^{2+}-triggered ROS-mediated SOD upregulation[50-51]. A 3.74-fold surge in MDA at 20% mortality ((34.50 ± 3.53) nmol/mgprot, $P<0.001$) signaled Cu^{2+}-driven lipid peroxidation[52]. Despite a 64% decline in MDA at 50% mortality, significant tissue damage persisted, evidenced by membrane rupture and connective tissue vacuolization in gills and gonads. GST remained hyperactive ((5.72-7.81) U/mgprot, $P<0.001$), conjugating glutathione (GSH) with Cu^{2+} to mitigate toxicity[53], though this defense faltered at advanced mortality stages. AChE transiently increased at 50% mortality ($P<0.01$)—likely a compensatory response to SDH-suppressed mitochondrial energy production during peak shell-closure stress, as acetylcholine signaling supports adductor muscle contraction[54].

3.4 NaClO-Induced Responses

L. fortunei mounted a robust self-protection response against NaClO: SDH activity increased to 1.5 times that of the control. This elevation corresponded to a period of prolonged shell closure, which limited ClO^- influx and thereby helped preserve gill integrity up to 50% mortality. SOD rose modestly (peak (11.67 ± 1.13) U/mgprot at 70% mortality), while MDA remained suppressed at 50% mortality ((4.73 ± 0.56) nmol/mgprot) before spiking at 70% mortality ((26.28 ± 2.12) nmol/mgprot), signaling delayed oxidative damage upon shell reopening. GST showed a fluctuative pattern: it was first induced at 50% mortality and then decreased at 70% mortality, likely due to ClO^--induced disruption of GST biosynthesis that overwhelmed the antioxidant capacity[55]. Collectively, NaClO toxicity stems from dual mechanisms: initial membrane damage via ClO^- oxidation, compounded by late-stage oxidative stress when self-protection (shell closure) fails[56].

4 Conclusion

The main conclusions of this study are as follows:

(1) Among the eight tested agents ($CuSO_4$, chloramine, salicylic acid, glyphosate, chitosan-based flocculant, NaClO, NS, and polyquaternium), the three most effective against *L. fortunei* were NS (2 mg/L), $CuSO_4$ (1 mg/L) and NaClO (3 mg/L).

(2) NS induced toxicity through dual pathways: (i) causing oxidative damage to gill and gonad tissues; and (ii) inhibiting AChE, a mechanism akin to that of organophosphorus pesticides, leading to combined oxidative stress, mitochondrial dysfunction, and neurotoxicity. $CuSO_4$ mediated toxicity through Cu^{2+} diffusion and ion exchange, promoting lipid peroxidation and membrane integrity; however, *L. fortunei* activated glutathione-dependent detoxification to mitigate Cu^{2+} toxicity. NaClO initially triggered rapid shell closure (within 30 min), during which antioxidant enzymes (SOD, GST) buffered ClO^--induced oxidative stress. However, at higher concentrations (≥4 mg/L), irreversible membrane damage and cytochrome c release triggered cellular apoptosis.

(3) For controlling *L. fortunei* biofouling in enclosed water systems including pipelines and hydraulic infrastructure, a targeted two-step strategy—application of $CuSO_4$, NS, or NaClO at recommended concentrations (1-3 mg/L) followed by removal of dead biomass may offer a viable emergency mitigation approach to prevent infrastructure damage caused by mussel proliferation.

References

[1] Xu M Z. Distribution and spread of *Limnoperna fortunei* in China[M]//*Limnoperna fortunei*. Cham: Springer International Publishing, 2015: 313-320.

[2] Oliveira M D, Campos M C S, Paolucci E M, *et al*. Colonization and spread of *Limnoperna fortunei* in south America [M]//*Limnoperna fortunei*. Cham: Springer International Publishing, 2015: 333-355.

[3] Ito K. Colonization and spread of *Limnoperna fortunei* in Japan[M]//*Limnoperna fortunei*. Cham: Springer International Publishing, 2015: 321-332.

[4] Luo F M, Zhang Z Z, Hu X P. Reproduction laws of *Limnoperna fortunei* in the raw water pipelines of Shenzhen city [J]. *Sci-tech Economic Market*, 2009(3): 109-110(Ch).

[5] Morton B. The reproductive cycle in *Limnoperna fortunei* (Dunker 1857) (Bivalvia: Mytilidae) fouling Hong Kong's raw water supply system[J]. *Oceanol Limnol Sinica*, 1982, **13**: 312-324.

[6] Yao G Y, Xu M Z, An X H. Concrete deterioration caused by freshwater mussel *Limnoperna fortunei* fouling[J]. *International Biodeterioration and Biodegradation*, 2017, **121**: 55-65.

[7] Ou Z X. *Study on the Influence of Limnoperna fortunei on the Water Conveyance Capacity of Channels*[D]. Handan: Hebei University of Engineering, 2020(Ch).

[8] Liu Z P, Jian Y Z, Xia Y D. Preliminary exploration of the hazards and treatment measures of *Limnoperna fortunei*: A case study of Nuozhadu Hydropower Station[C]//*Proceedings of the* 2021 *Technical Supervision Work Exchange Meeting and Professional Technical Forum of the Electric Power Industry*. Beijing: China Electric Power Press, 2021: 746-751(Ch).

[9] Li R, Wang H S, Bai J C, *et al*. Habitat analysis of *Limnoperna fortunei* in Beitang reservoir in Tianjin[J]. *Water Technology*, 2020, **14**(1): 19-22(Ch).

[10] Zhang J H, Xu M Z, Sun L, *et al*. Impact of golden mussel (*Limnoperna fortunei*) colonization on bacterial communities and potential risk to water quality[J]. *Ecological Indicators*, 2022, **144**: 109499.

[11] dos Santos R N, Campos F S, de Albuquerque N R M, *et al*. A new marseillevirus isolated in southern Brazil from *Limnoperna fortunei*[J]. *Scientific Reports*, 2016, **6**: 35237.

[12] Wang R N, Wang X L, Li S M, *et al*. Study on the law of harmful gas release from *Limnoperna fortunei* (Dunker 1857) during maintenance period of water tunnel based on K-means outlier treatment[J]. *Applied Sciences*, 2021, **11** (24): 11995.

[13] Zhang R H, Zhang Y H, Fei X L, *et al*. *Limnoperna fortunei* as an invasive biofouling bivalve species in freshwater: A review of its occurrence, biological traits, risks, and control strategies[J]. *Journal of Water Supply*: *Research and Technology-Aqua*, 2022, **71**(12): 1364-1383.

[14] Matsui K, Fumoto T, Kawakami H. Testing the repellent effects of construction materials on the attachment of the invasive golden mussel, *Limnoperna fortunei*, in a Japanese urban tidal river[J]. *Limnology*, 2019, **20**(1): 131-136.

[15] Paolucci E M, Ron L, Thuesen E V. Metabolic response to increasing environmental temperature in the invasive mussel *Limnoperna fortunei*[J]. *Austral Ecology*, 2022, **47**(4): 818-827.

[16] Perepelizin P V, Boltovskoy D. Control of *Limnoperna fortunei* fouling by oxygen deprivation[M]//*Limnoperna fortunei*. Cham: Springer International Publishing, 2015: 451-454.

[17] Zhu Y Z, Yang H W, Zhou L. Construction and application of an underwater cleaning system for *Limnoperna fortunei* based on cavitation jet technology[J]. *China Water Transport*, 2022, **22**(12): 53-55(Ch).

[18] Li R, Jia X Z, Hu J K, *et al*. Research on the elimination of *Limnoperna fortunei* by chemical agents[J]. *Water Supply Technology*, 2021, **15**(1): 29-32(Ch).

[19] Miranda C E, Clauser C D, Lozano V L, *et al*. An invasive mussel is in trouble: How do glyphosate, 2, 4-D and its mixture affect *Limnoperna fortunei*'s survival?[J]. *Aquatic Toxicology*, 2021, **239**: 105957.

[20] Luo F M, Liu L J, You Z L, *et al*. Study on solvability of *Limnoperna fortunei* byssus cohering in raw water pipe[J]. *Water & Wastewater Engineering*, 2006, **42**(3): 29-32(Ch).

[21] Silva I, Naya D, Teixeira de Mello F, *et al*. Fish *vs*. Aliens: Predatory fish regulate populations of *Limnoperna fortunei* mitigating impacts on native macroinvertebrate communities [J]. *Hydrobiologia*, 2021, **848**(9): 2281-2301.

[22] Rosa D M, Santos G B, Gomes P L A, *et al*. Occurrence of *Limnoperna fortunei* (Dunker 1857) in the fish diet from a south-eastern Brazilian reservoir[J]. *Journal of Applied Ichthyology*, 2015, **31**(1): 188-191.

[23] Hong J. *Study on the Hazard Characteristics and Control Measures of Limnoperna fortunei in Water Conveyance Pipelines*[D]. Harbin: Harbin Institute of Technology, 2012(Ch).

[24] Li S G, Chen Y Y, Gao Y C, *et al*. Chemical oxidants affect byssus adhesion in the highly invasive fouling mussel *Limnoperna fortunei*[J]. *Science of the Total Environment*, 2019, **646**: 1367-1375.

[25] Jin X W, Zha J M, Xu Y P, *et al*. Toxicity and oxidative stress of three chlorophenols to freshwater clam corbicula fluminea[J]. *Asian Journal of Ecotoxicology*, 2009, **4**(6):

816-822(Ch).

[26] Mao G Y, Zhou H R, Huang Y, *et al*. Analysis of glutathione S-transferase gene expression in *Pomacea canaliculata* under Cu^{2+} stress[J]. *Chinese Journal of Parasitology and Parasitic Diseases*, 2019, **37**(2): 213-217, 231(Ch).

[27] Liu H M, Dong Y H, Huo L H, *et al*. Acute toxicity of Cu^{2+} and its effects on antioxidant enzymes in Si-nonovacula constricta juveniles[J]. *Journal of Fishery Sciences of China*, 2012, **19**(1): 182-187(Ch).

[28] Jiao W, Zhou W Q, Zhang W, *et al*. Research progress on detection methods of acetylcholinesterase[J]. *Biochemical Engineering*, 2023, **9**(5): 201-203.

[29] Li D L, Dong S S, Li D D, *et al*. Burrowing behavior and physiological responses of the cockle (*Clinocardium californiense*) to different substrates[J]. *Chinese Fishery Quality and Standards*, 2019, **9**(2): 24-31(Ch).

[30] Rajagopal S, Nair K V K, Azariah J, *et al*. Chlorination and mussel control in the cooling conduits of a tropical coastal power station[J]. *Marine Environmental Research*, 1996, **41** (2): 201-221.

[31] Boukadida K, Cachot J, Clérandeaux C, *et al*. Early and efficient induction of antioxidant defense system in *Mytilus galloprovincialis* embryos exposed to metals and heat stress[J]. *Ecotoxicology and Environmental Safety*, 2017, **138**: 105-112.

[32] Wang R. *Study on the Oxidative Killing and Removal Technology of Limnoperna fortunei in Long-distance Water Transmission Pipelines*[D]. Harbin: Harbin Institute of Technology, 2013(Ch).

[33] Zhou Y, Raphael R M. Effect of salicylate on the elasticity, bending stiffness, and strength of SOPC membranes[J]. *Biophysical Journal*, 2005. **89**(3): 1789-1801.

[34] Gattás F, Espinosa M, Babay P, *et al*. Invasive species versus pollutants: Potential of *Limnoperna fortunei* to degrade glyphosate-based commercial formulations[J]. *Ecotoxicology and Environmental Safety*, 2020, **201**: 110794.

[35] de Stefano L G, Gattás F, Vinocur A, *et al*. Comparative impact of two glyphosate-based formulations in interaction with *Limnoperna fortunei* on freshwater phytoplankton[J]. *Ecological Indicators*, 2018, **85**: 575-584.

[36] Pizarro H, Di Fiori E, Sinistro R, *et al*. Impact of multiple anthropogenic stressors on freshwater: How do glyphosate and the invasive mussel *Limnoperna fortunei* affect microbial communities and water quality? [J]. *Ecotoxicology*, 2016, **25**(1): 56-68.

[37] Flórez Vargas R P, Saad J F, Graziano M, *et al*. Bacterial composition of the biofilm on valves of *Limnoperna fortunei* and its role in glyphosate degradation in water[J]. *Aquatic Microbial Ecology*, 2019, **83**(1): 83-94.

[38] Chen F M, Liu W, Pan Z B, *et al*. Characteristics and mechanism of chitosan in flocculation for water coagulation in the Yellow River diversion reservoir[J]. *Journal of Water Process Engineering*, 2020, **34**: 101191.

[39] Claudi R, de Oliveira M D. Chemical strategies for the control of the golden mussel (*Limnoperna fortunei*) in industrial facilities[M]//*Limnoperna fortunei*. Cham: Springer International Publishing, 2015: 417-441.

[40] Ni H J, Zhang Q M, Guo Y D. Experiment on removal of *Limnoperna fortunei* from raw water pipe wall by soaking method of NaClO[J]. *Water Purification Technology*, 2021, **40**(5): 131-134(Ch).

[41] Lu X, Wang C, Liu B Z. The role of Cu/Zn-SOD and Mn-SOD in the immune response to oxidative stress and pathogen challenge in the clam *Meretrix meretrix*[J]. *Fish & Shellfish Immunology*, 2015, **42**(1): 58-65.

[42] Winston G W, di Giulio R T. Prooxidant and antioxidant mechanisms in aquatic organisms[J]. *Aquatic Toxicology*, 1991, **19**(2): 137-161.

[43] Rosic N N, Pernice M, Dunn S, *et al*. Differential regulation by heat stress of novel cytochrome P450 genes from the dinoflagellate symbionts of reef-building corals[J]. *Applied and Environmental Microbiology*, 2010, **76**(9): 2823-2829.

[44] Wang X W, Xiao S S, Zhang R, *et al*. Physiological changes and transcriptional modulation of *HIF-αs* in Siberian sturgeon in response to hypoxia[J]. *Aquaculture*, 2021, **545**: 737219.

[45] Moosavi B, Berry E A, Zhu X L, *et al*. The assembly of succinate dehydrogenase: A key enzyme in bioenergetics[J]. *Cellular and Molecular Life Sciences*, 2019, **76**(20): 4023-4042.

[46] Chiang P K, Bourgeois J G, Bueding E. Histochemical distribution of acetylcholinesterase in the nervous system of the snail, biomphalaria glabrata[J]. *International Journal of Neuroscience*, 1972, **3**(2): 47-60.

[47] Ma J G, Zhang B J, Li X Y. Biochemistry response of physa acuta to chlorpyrifos toxicity[J]. *Journal of Hydroecology*, 2012, **33**(5): 114-118(Ch).

[48] Zhang R X, Li B H, Xu J Z. Determination of serum acetylcholinesterase activity in patients with myasthenia gravis and its clinical significance[J]. *Journal of Practical Medicine*, 2005, **21**(1): 2(Ch).

[49] Medithi S, Kasa Y D, Jee B, *et al*. Organophosphate pesticide exposure among farm women and children: Status of micronutrients, acetylcholinesterase activity, and oxidative stress[J]. *Archives of Environmental & Occupational Health*, 2022, **77**(2): 109-124.

[50] Li Y F, Gu Z Q, Liu H, *et al*. Biochemical response of the mussel *Mytilus coruscus* (Mytiloida: Mytilidae) exposed to *in vivo* sub-lethal copper concentrations[J]. *Chinese Journal of Oceanology and Limnology*, 2012, **30**(5): 738-745.

[51] Rossi F, Palombella S, Pirrone C, *et al*. Evaluation of tissue morphology and gene expression as biomarkers of pollution in mussel *Mytilus galloprovincialis* caging experiment[J]. *Aquatic Toxicology*, 2016, **181**: 57-66.

[52] Chan C Y, Wang W X. A lipidomic approach to understand copper resilience in oyster *Crassostrea hongkongensis*[J]. *Aquatic Toxicology*, 2018, **204**: 160-170.

[53] Chi C, Giri S S, Jun J W, *et al*. Marine toxin okadaic acid affects the immune function of bay scallop (*Argopecten irradians*)[J]. *Molecules*, 2016, **21**(9): 1108.

[54] Franco-Martinez L, Romero D, García-Navarro J A, *et al*. Measurement of p-nitrophenyl acetate esterase activity (EA), total antioxidant capacity (TAC), total oxidant status (TOS) and acetylcholinesterase (AChE) in gills and digestive gland of *Mytilus galloprovincialis* exposed to binary mixtures of Pb, Cd and Cu[J]. *Environmental Science and Pollution Research*, 2016, **23**(24): 25385-25392.

[55] Xia L P, Chen S H, Dahms H U, *et al*. Cadmium induced oxidative damage and apoptosis in the hepatopancreas of *Meretrix meretrix*[J]. *Ecotoxicology*, 2016, **25**(5): 959-969.

[56] Ban N, Takahashi Y, Takayama T, *et al*. Transfection of glutathione S-transferase (GST) -pi antisense complementary DNA increases the sensitivity of a colon cancer cell line to adriamycin, cisplatin, melphalan, and etoposide[J]. *Cancer Research*, 1996, **56**(15): 3577-3582.

常见化学药剂对水利工程中淡水壳菜的防治效果及作用机理

刘坚[1,2]， 陈正虎[3]， 蔡伟[3]， 王英才[1,2]， 田娜娜[1,2]， 郭文思[1,2]， 李天翠[1,2†]

1. 生态环境部长江流域生态环境监督管理局 生态环境监测与科学研究中心，湖北 武汉 430010

2. 生态环境部长江流域水生生物监测与评估重点实验室（筹），湖北 武汉 430010

3. 中国长江电力股份有限公司，湖北 宜昌 430014

摘要：淡水壳菜（*Limnoperna fortunei*）是水利工程中常见的污损生物，化学药剂灭杀是去除淡水壳菜的常用方法。本文研究了$CuSO_4$、氯胺、NaClO、水杨酸、草甘膦、壳聚糖基絮凝剂、硫酸烟酰苯胺盐（以下简称NS）和聚季铵盐八种化学药剂对淡水壳菜的灭杀效果和机理。结果表明，毒性效果由高到低依次为：NS > $CuSO_4$ > NaClO>聚季铵盐＞水杨酸＞草甘膦＞氯胺＞壳聚糖基絮凝剂。其中，NS（2 mg/L）、$CuSO_4$（1 mg/L）、NaClO（3 mg/L）这三种药剂对淡水壳菜的灭杀效果较好，死亡率达73%以上。测定了三种药剂作用后不同死亡率下淡水壳菜酶活含量，结果发现，NS、$CuSO_4$、NaClO对淡水壳菜生理生化指标的影响存在显著差异。NS作用淡水壳菜时，超氧化物歧化酶（SOD）和谷胱甘肽S-转移酶（GST）随死亡率升高持续增强，丙二醛（MDA）在死亡率70%时明显升高，琥珀酸脱氢酶（SDH）均显著低于对照组，乙酰胆碱酯酶（AChE）略有升高后降低。$CuSO_4$作用淡水壳菜时，不同死亡率下SOD持续升高，MDA、GST剧烈波动，SDH抑制趋势与NS类似，AChE在50%死亡率时升高。NaClO处理淡水壳菜时，SOD轻度升高，MDA剧增，GST先升高后降低，SDH在死亡率为70%时升高，AChE在死亡率50%时升高。这说明NS和$CuSO_4$可能是由氧化应激和线粒体抑制来抑制淡水壳菜机体活性，而NaClO直接通过膜损伤与晚期氧化损伤作用来胁迫机体。死亡率达到50%、70%时对淡水壳菜的鳃丝及性腺进行染色切片观察。NS作用后鳃丝形态异常、细胞分布紊乱，性腺萎缩空化；$CuSO_4$作用后鳃丝萎缩、性腺破损严重，结缔组织空化明显；NaClO在死亡率为50%时对腮丝和性腺影响较小，但在死亡率为70%时鳃丝细胞减少、顶端空洞，性腺空化明显，核消失。组织病理学观察显示，三种化学药剂作用会导致淡水壳菜鳃丝结构紊乱、性腺萎缩空化，甚至细胞核消失，造成明显的组织损伤。本研究为水利工程管道和封闭结构中化学药剂灭杀淡水壳菜（如NS、$CuSO_4$和NaClO等）的选择提供了理论依据。

关键词：淡水壳菜（*Limnoperna fortunei*）；化学药剂；酶活；HE染色

□